PARAMETRIC ANALYSIS FOR THE DESIGN OF A 4 POLE RADIAL PERMANENT MAGNET GENERATOR FOR SMALL WIND TURBINES*

ROBERTO QUINTAL-PALOMO, MATEUSZ DYBKOWSKI, MACIEJ GWOŹDZIEWICZ

Wrocław University of Science and Technology, Department of Electrical Machines,
Drives and Measurements, ul. Smoluchowskiego 19, 50-370 Wrocław, Poland,
e-mail: roberto.quintal@pwr.edu.pl

Abstract: A review of the literature gives several guidelines for the design of a Permanent Magnet Synchronous Generator (PMSG) for Small Wind Turbines (SWT) applications. This paper presents Finite Element Analysis (FEA) of a Surface Mounted PMSG. Several optimization tests are run in order to yield the lowest Total Harmonic Distortion (THD) and cogging torque with the highest induced voltage. The results of the optimization tests are then utilized to design an initial "optimized" circumferential Internal PMSG. This optimized design is then compared to a non-optimized design, as well as the results of the Surface Mounted PMSG.

Keywords: *permanent magnet synchronous generator PMSG, finite element analysis FEA, small wind turbines SWT*

1. INTRODUCTION

1.1. PERMANENT MAGNET GENERATOR TOPOLOGIES

The focus on high efficiency, renewable energy and applications, such as the electric vehicles (EVs) or hybrid electric vehicles (HEVs), have brought more attention to the area of electrical machine design. This attention has brought a renewed effort in the study and classification of the electrical machine topologies [1]–[5]. This manuscript centers on the permanent magnet machine and its rotor configurations.

A common classification guide for the PMSG is presented in Figs. 1 and 2.

The overlapping distributed stator winding is analyzed using both the Surface Permanent Magnet (SPM) and the circumferential Internal Permanent Magnet (IPM).
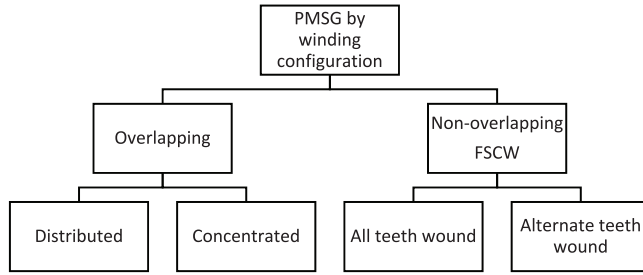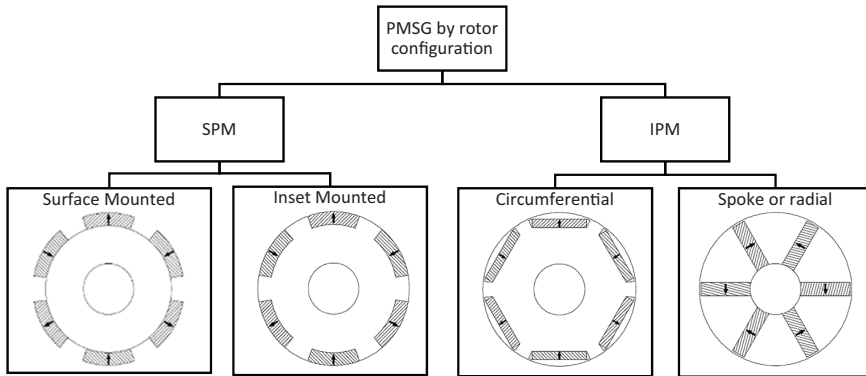

Fig. 1. Radial PMSG stator topologies [6]

Fig. 2. Radial PMSG rotor topologies [7]

In the paper, the PMSG machine was created based on the Induction Motor (IM): stator and housing of a three phase 1.5 kW, 1500 rpm. It has 36 slots in the stator and was designed with a 0.5 mm airgap to have a compact form factor as shown in Fig. 3. Since the rotor diameter is small, the machine has 4 poles.
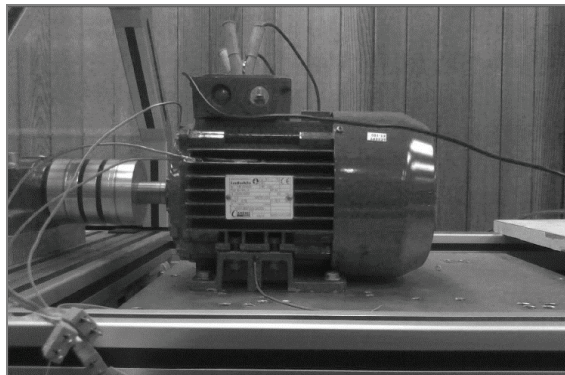

Fig. 3. The Sh90 L-4 motor used as basis for the generator

Relevant literature shows that for slow-speed direct drive wind turbine application of a higher number of poles is desirable [8]–[10]. Nevertheless, advances in gearbox technology, e.g., Continuous Variable Transmission (CVT), Infinitely Variable Transmission (IVT) and magnetic gears [11]–[15], may return focus to these well studied and mass-produced electrical machines.

Another advantage of using an IM as a basis is the high reliability of this type of machines due to standard manufacturing processes and mass-production. Non-standard manufacturing processes have shown to be a source of faults in high power Wind Turbines (WTs) [16] and in low power SWTs [17] with new designs of direct drive slow speed generators.

1.2. THE SURFACE MOUNTED PERMANENT MAGNET GENERATOR FEA MODEL

A 2D model for the surface mounted PMSG is presented in Fig. 4. It should be noted that there are three geometrical dimensions subject to optimization. The "Embrace" is the percentage of the arch that corresponds to each magnet pole (90° is 100% in this case). The magnet "Thickness" is the maximum height of each magnet from the rotor iron to the airgap. The "Offset" is the center of the arch that forms the outer face of the magnet (airgap side). Note that only half of the PMSG is modeled because of symmetry considerations, which cuts down simulation time and computer memory during FEA. Also, note that the offset dimension has an effect not only on the geometry but also on the magnetization vector.
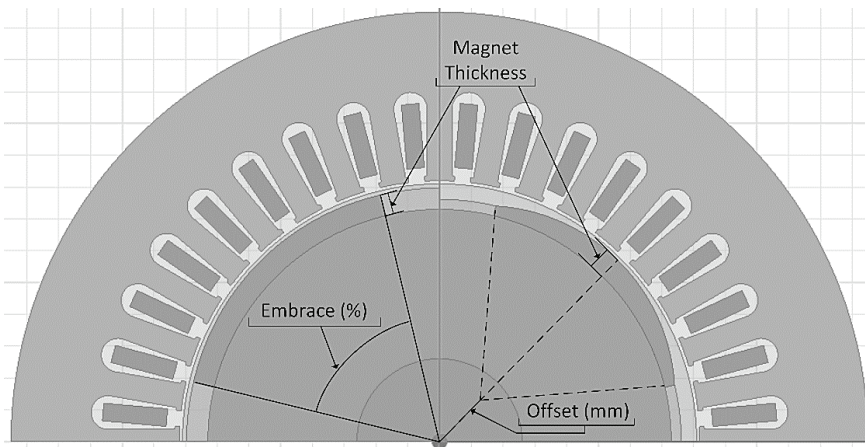

Fig. 4. The 2D model for finite element analysis FEA of the SM PMSG

The curved shape of the surface magnets is used for cogging torque minimization as shown in [18] and [19]. Cogging torque minimization is crucial for direct

drive PMSG in SWT due to its impacts on the turbine aerodynamics and the overall system efficiency moving the "cut-in speed" of the turbine's generator further (higher wind speed is needed) than intended by the aerodynamic blade design. The efficiency loss due to the sum of cogging torque and friction could be as much as 30% as shown in [20].

2. PARAMETRIC ANALYSIS

2.1. GEOMETRY VARIATIONS

From the three dimensions shown in Fig. 4, only embrace and offset are parametrically analyzed since it is evident that the magnet thickness is directly proportional to the induced voltage and the thicker the magnet, the higher the voltage induced in the terminals. For economical and practical purposes for a future construction stage, a 4 mm magnet thickness was fixed.

Two cases were studied: symmetrical and asymmetrical. As observed in Fig. 4, only two poles of the four pole machine are modeled. This allows for the analysis of the variation of 2 poles of the whole machine (asymmetrical case) and the variation of all 4 poles at the same time (symmetrical case). Therefore, in the model shown in Fig. 4, for the asymmetrical case, only one pole is being modified, that is, 2 poles of the complete machine are being modified.
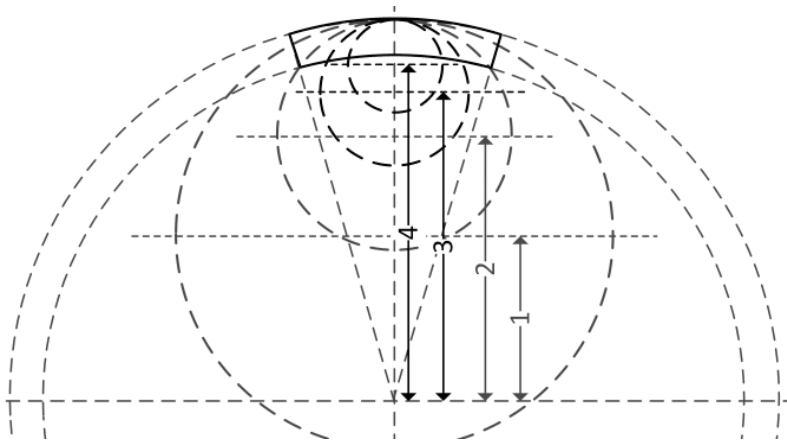

Fig. 5. Four different offsets for a fixed embrace

At every variation step the model was simulated in transient conditions (time dependent) for the nominal 1500 rpm speed using the FEA software Maxwell from ANSYS[®].

The embrace was varied from 30 to 90% in 10% steps, and the offset was fixed to 0 mm. Figure 6 shows the spectral analysis results for the symmetrical embrace variation. In this figure, the Fast Fourier Transform (FFT) of the induced voltage in one phase is shown. Also, for this case, the 70% embrace variation is marked with an arrow because it has the highest fundamental induced voltage (first and tallest column) and the lowest induced harmonics (multiples of 50 Hz).
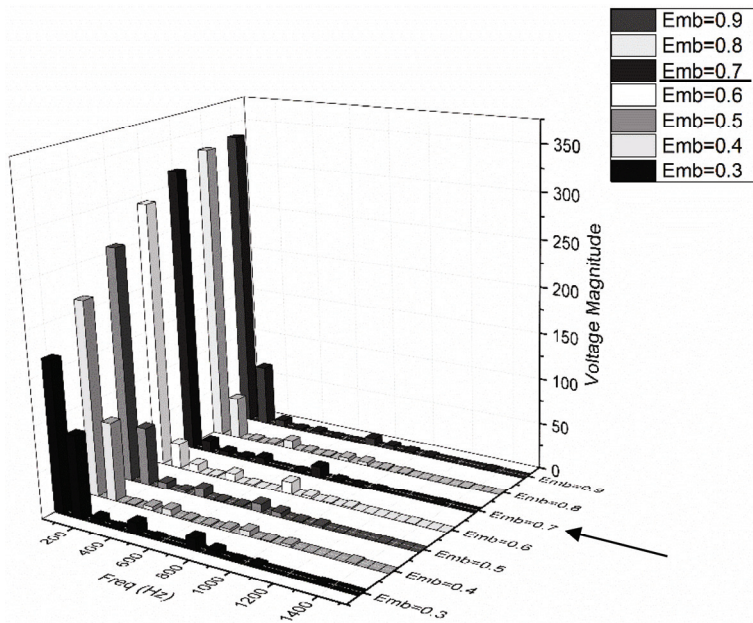

Fig. 6. Spectral analysis of symmetrical embrace

Figure 7 shows the results for the asymmetrical embrace variation. Here, a 60% embrace is marked. It has almost the same fundamental amplitude (328 V) as the 0.9 embrace (352 V) but lower harmonics.

A variation in offset after choosing the embrace was done because is less prone to produce invalid geometries. In Fig. 5, the offset 4 and 3 would create an invalid geometry because the arch is smaller than the embrace. Therefore, the offset 2 is the largest offset available for this embrace and it can be varied from 0 to offset 2.

The offset was then varied from 1 to 11 mm in 1 mm steps with a fixed 0.7 embrace. This embrace was chosen because of the higher induced voltage and lowest THD in the symmetrical case for 0.7 embrace, as shown in Fig. 6 and Fig. 10a. The results of the offset variation can be seen in Fig. 8 for symmetrical case and Fig. 9 for asymmetrical case.
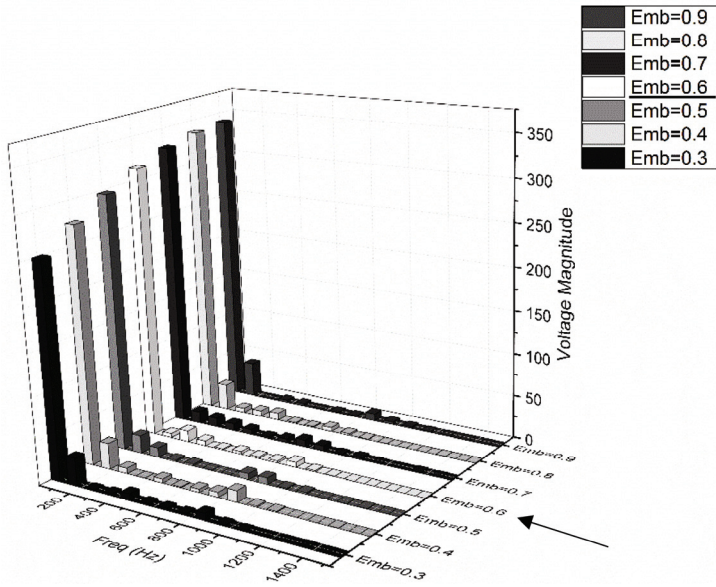
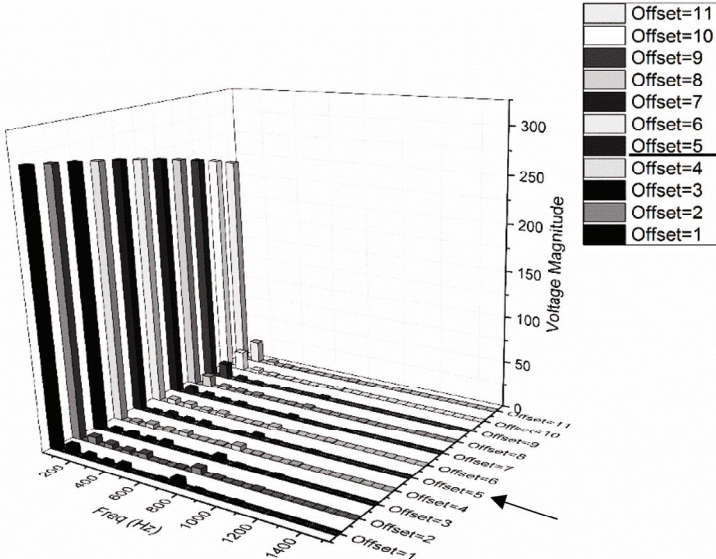Fig. 7. Spectral analysis of asymmetrical embrace

Fig. 8. Spectral analysis of the symmetric offset variation

The results for the symmetrical offset variation in Fig. 8 show that the 5 mm offset offers the lowest harmonics but also shows that the magnet curved shape comes at the expense of an induced phase voltage drop to about 275 V.
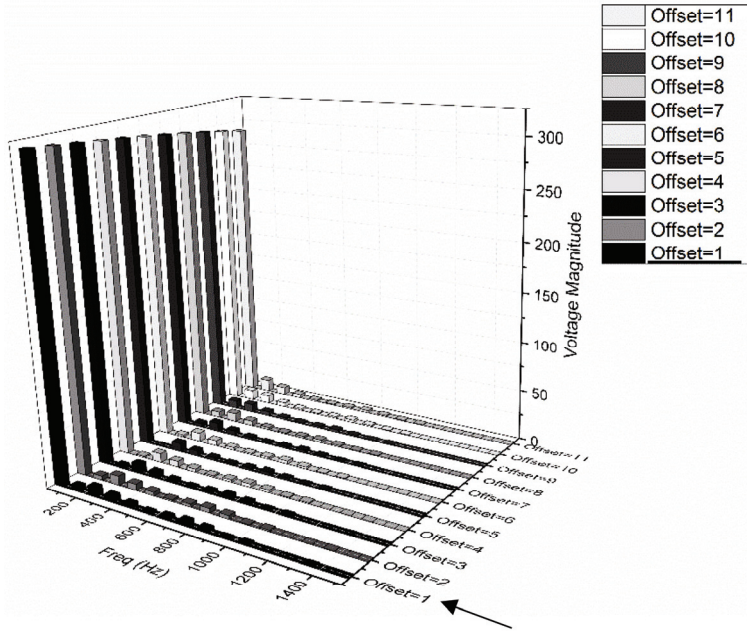
Fig. 9. Spectral analysis of the asymmetric offset variation

2.2. TOTAL HARMONIC DISTORTION AND LINE VOLTAGE

Even though some parameters are clear in the spectral analysis some figures of merit were calculated from the 2D model for better assessment. The Total Harmonic Distortion (THD) was calculated using the following equation

$$THD = \frac{\sqrt{V_2^2 + V_3^2 + ... + V_N^2}}{V_1} \tag{1}$$

where V_1 is the magnitude of the fundamental frequency (50 Hz) and V_2 to V_N are the magnitudes of the harmonics.

The THD was calculated from the spectral analysis using harmonics up to and including 1.5 kHz (30th harmonic). This calculation had to be performed outside the Maxwell software due to the harmonic manual extraction.

The results of the embrace variation, with 0 mm offset, are presented in Fig. 9. For the symmetric case, a 0.7 embrace gives the lowest THD at an induced line voltage of 424 V rms.

For the asymmetric case 0.5 embrace gives the lowest THD but at an induced line voltage of 357 V rms only. Therefore, an embrace of 0.6 is preferred because its THD is still below 10% and has an induced line voltage of 379 V rms.
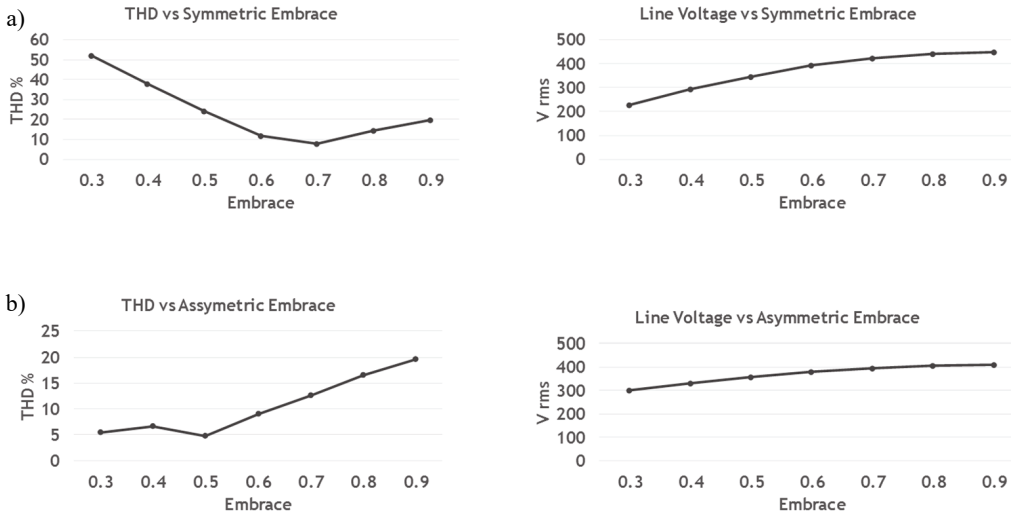
a)

THD vs Symmetric Embrace

Line Voltage vs Symmetric Embrace

Fig. 10. Embrace variation THD and induced line voltage for (a) symmetric and (b) asymmetric case

a)

THD vs Symmetric Offset

Line Voltage vs Symmetric Offset

b)

THD vs Asymmetric Offset

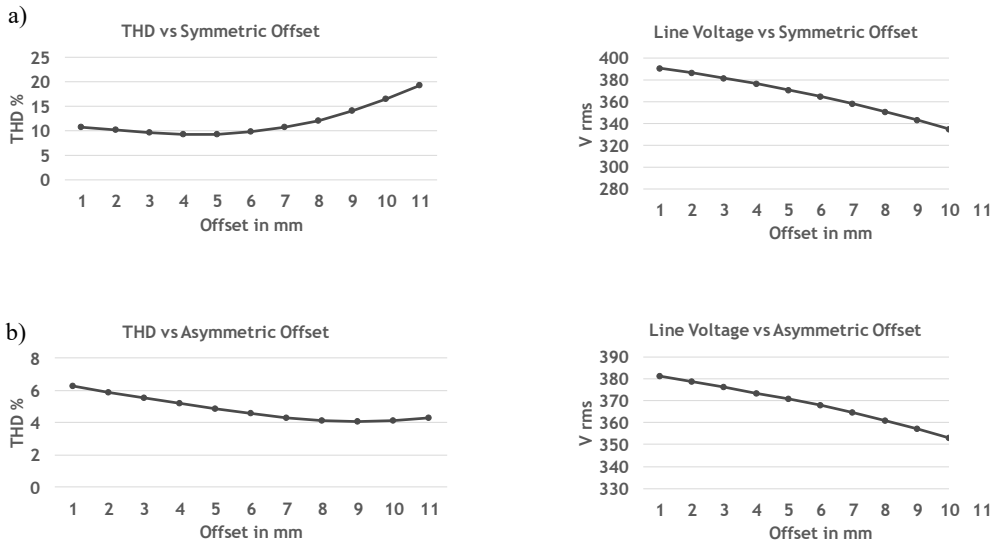Line Voltage vs Asymmetric Offset

Fig. 11. Offset variation THD and induced line voltage for (a) symmetric and (b) asymmetric case

The offset's variation results are presented in Fig. 11. Embrace is fixed at 0.7. An offset of 5 mm has the lowest THD for the symmetric case with an induced voltage of 371 V rms. An offset of 1mm is preferred in the asymmetric case with 381 V rms line voltage, because the THD is already below 10% and the induced line voltage-trend has a very steep slope.

3. RESULTS

3.1. INTERNAL PERMANENT MAGNET

Based on the surface analysis, the symmetric case with a 0.7 embrace and 5 mm offset was chosen as template for the rotor shape of the IPMSG design. In Fig. 12, the SPM and IPM models are shown. Notice that the rotor of Fig. 12b does not have a circular shape, it has an arch given by the 5 mm offset instead. The IPM design has the advantage of using off the shelf rectangular magnets readily available from many suppliers. No special magnet manufacturing is needed, thus lowering the costs for future construction. Also, it is important to mention that the SPM design has 132 mm^2 of area of one magnet and the IPM design has 200 mm^2 area of one magnet.
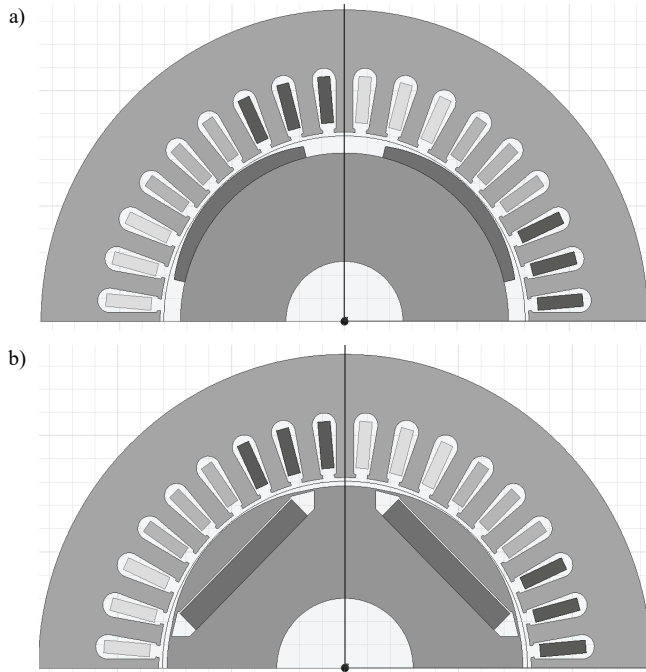

Fig. 12. (a) Selected SPM model, (b) IPM model based on the SPM shape

The IPM design shown in Fig. 12b obtained 414 V rms of line induced voltage with a 6.29% THD and 0.48 Nm cogging torque at nominal load. This last figure of merit is of most importance for direct drive SWTs and the goal for using an optimized shape on the rotor.

A comparison of the cogging torque for the chosen SPM and two IPM cases, non-optimized shape (circular rotor) and optimized shape, based on the SPM chosen is

presented in Fig. 13. These calculations were made using a 64 Ohm load (for obtaining nominal current) and 0.5 mm airgap between the rotor and the stator in all cases.
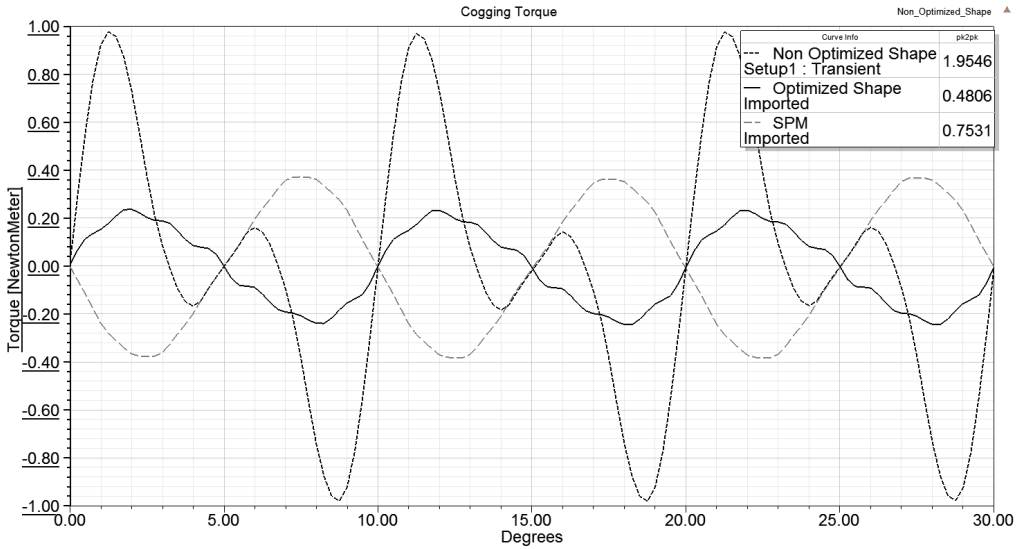

Fig. 13. Cogging torque for IPM non-optimized shape, optimized shape and the SPM chosen

3.1. CONCLUSIONS

The shape optimization of the IPMSG is possible using the SPM design as template for the rotor outer shape. Many efforts have been made in surface magnet shaping using different methods [21]–[23]. The manufacturing of special-shaped magnets makes them viable only for mass production. A method involving the SPM shape for the design of an IPMSG was presented.

Table 1. Results for the three models

	Optimized Surface Permanent Magnet	Internal Permanent Magnet without optimized shape	Internal Permanent Magnet with optimized shape
Induced back-EMF line voltage	424 V rms	426 V rms	414 V rms
Fundamental frequency 50 Hz magnitude	371 V rms	340 V rms	340 V rms
Total harmonic distortion in %	9.32%	22.19%	6.12%
Cogging torque	0.75 Nm	1.95 Nm	0.48 Nm
Magnet transversal area	132 mm^2	200 mm^2	200 mm^2

FEA predicts very good characteristics for an optimized shape IPMSG. Low cogging torque, high induced voltage, and low THD are desirable in SWT generators.

A trade-off between SPM and IPM generators is the amount of magnet volume needed to induce the same voltage on both. In the 2D model, a 51% bigger area was needed to obtain 414 V rms in comparison to the 424 V rms obtained with the SPM, as shown in Table 1.

3.2. FUTURE WORK

The designed IPMSG will be constructed to compare the FEA predicted characteristics with experimental measurements.

ACKNOWLEDGMENTS

REFERENCES

[1] MALINOWSKI M., MILCZAREK A., KOT R., GORYCA Z., SZUSTER J.T., *Optimized Energy-Conversion Systems for Small Wind Turbines: Renewable energy sources in modern distributed power generation systems*, IEEE Power Electronics Magazine, Sept. 2015, 2, 3, 16–30.

[2] WANG Y., XU L., *Peak Power Improvement of Interior Permanent Motor for Electrified Vehicles*, IEEE Electrification Magazine, June 2014, 2, 2, 25–30.

[3] EL-REFAIE A.M., *Motors/generators for traction/propulsion applications: A review*, IEEE Vehicular Technology Magazine, March 2013, 8, 1, 90–99.

[4] EL-REFAIE A.M., *Fault-tolerant permanent magnet machines: a review*, IET Electric Power Applications, January 2011, 5, 1, 59–74.

[5] POLINDER H., FERREIRA J.A., JENSEN B.B., ABRAHAMSEN A.B., ATALLAH K., MCMAHON R.A., *Trends in Wind Turbine Generator Systems*, IEEE Journal of Emerging and Selected Topics in Power Electronics, Sept. 2013, 1, 3, 174–185.

[6] EL-REFAIE A.M., *Fractional-slot concentrated-windings: A paradigm shift in electrical machines*, 2013 IEEE Workshop on, Electrical Machines Design Control and Diagnosis (WEMDCD), Paris 2013, 24–32.

[7] BERNATT J., GLINKA T., JAKUBIEC M., KROL E., ROSSA R., *Electric motors with permanent magnets with two-zone rotational speed control*, International Aegean Conference on Electrical Machines and Power Electronics, ACEMP '07, Bodrum, 2007, 653–658.

[8] SPOONER E., GORDON P., BUMBY J.R., FRENCH C.D., *Lightweight ironless-stator PM generators for direct-drive wind turbines*, IEE Proceedings – Electric Power Applications, 7 Jan. 2005, 152, 1, 17–26.

[9] TUTTELBERG K., VAIMANN T., KALLASTE A., *Analysis of a slow-speed slotless permanent magnet synchronous generator*, 4th International Youth Conference on Energy (IYCE), 2013, 1–5.

[10] VALAVI M., NYSVEEN A., NILSSEN R., LORENZ R.D., RØLVÅG T., *Influence of Pole and Slot Combinations on Magnetic Forces and Vibration in Low-Speed PM Wind Generators*, IEEE Transactions on Magnetics, May 2014, 50, 5, 1–11.

[11] ROSSI C., CORBELLI P., GRANDI G., *W-CVT continuously variable transmission for wind energy conversion system*, Power Electronics and Machines in Wind Applications, PEMWA 2009, IEEE, Lincoln, NE, 2009, 1–10.

[12] [Online] Available: https://www.technologyreview.com/s/416038/testing-cheap-wind-power/

[13] JORGENSEN F.T., ANDERSEN T.O., RASMUSSEN P.O., *The Cycloid Permanent Magnetic Gear*, IEEE Transactions on Industry Applications, Nov.–Dec. 2008, 44, 6, 1659–1665.

[14] ATALLAH K., WANG J., CALVERLEY S.D., DUGGAN S., *Design and Operation of a Magnetic Continuously Variable Transmission*, IEEE Transactions on Industry Applications, July–Aug. 2012, 48, 4, 1288–1295.

[15] GERBER S., WANG R.J., *Design and Evaluation of a Magnetically Geared PM Machine*, IEEE Transactions on Magnetics, Aug. 2015, 51, 8, 1–10.

[16] TAVNER P.J., SPINATO F., VAN BUSSEL G., KOUTOULAKOS E., *Reliability of Different Wind Turbine Concepts with Relevance to Offshore Application*, European Wind Energy Conference, Scientific Track, Brussels, Belgium, European Wind Energy Association, April 2008.

[17] KALLASTE A., VAIMANN T., BELAHCEN A., *Possible manufacturing tolerance faults in design and construction of low speed slotless permanent magnet generator*, 16th European Conference on Power Electronics and Applications (EPE'14-ECCE Europe), Lappeenranta, 2014, 1–10.

[18] MULJADI E., GREEN J., *Cogging Torque Reduction in a Permanent Magnet Wind Turbine Generator*, 21st American Society of Mechanical Engineers ASME, Wind Energy Symposium, Reno, Nevada, January 14–17, 2002.

[19] CHUNG D., YOU Y., *Cogging Torque Reduction in Permanent-Magnet Brushless Generators for Small Wind Turbines*, Journal of Magnetics, 2015, 20(2), 176–185.

[20] ROLAK M., KOT R., MALINOWSKI M., GORYCA Z., SZUSTER J.T., *Design of Small Wind Turbine with Maximum Power Point Tracking Algorithm*, IEEE International Symposium on Industrial Electronics, Gdańsk, 2011, 1023–1028.

[21] UPADHAYAY P., RAJAGOPAL K.R., *Torque ripple reduction using magnet pole shaping in a surface mounted Permanent Magnet BLDC motor*, International Conference on Renewable Energy Research and Applications (ICRERA), Madrid, 2013, 516–521.

[22] WANG K., ZHU Z.Q., OMBACH G., *Torque Improvement of Five-Phase Surface-Mounted Permanent Magnet Machine Using Third-Order Harmonic*, IEEE Transactions on Energy Conversion, Sept. 2014, 29, 3, 735–747.

[23] ILKA R., ALINEJAD-BEROMI Y., YAGHOBI H., *Geometry optimization of five-phase permanent magnet synchronous motors using Bees algorithm*, IJEEE Iranian Journal of Electrical & Electronic Engineering, 2015, 11(4), 345–353.